SUPPLEMENTAL FIGURES

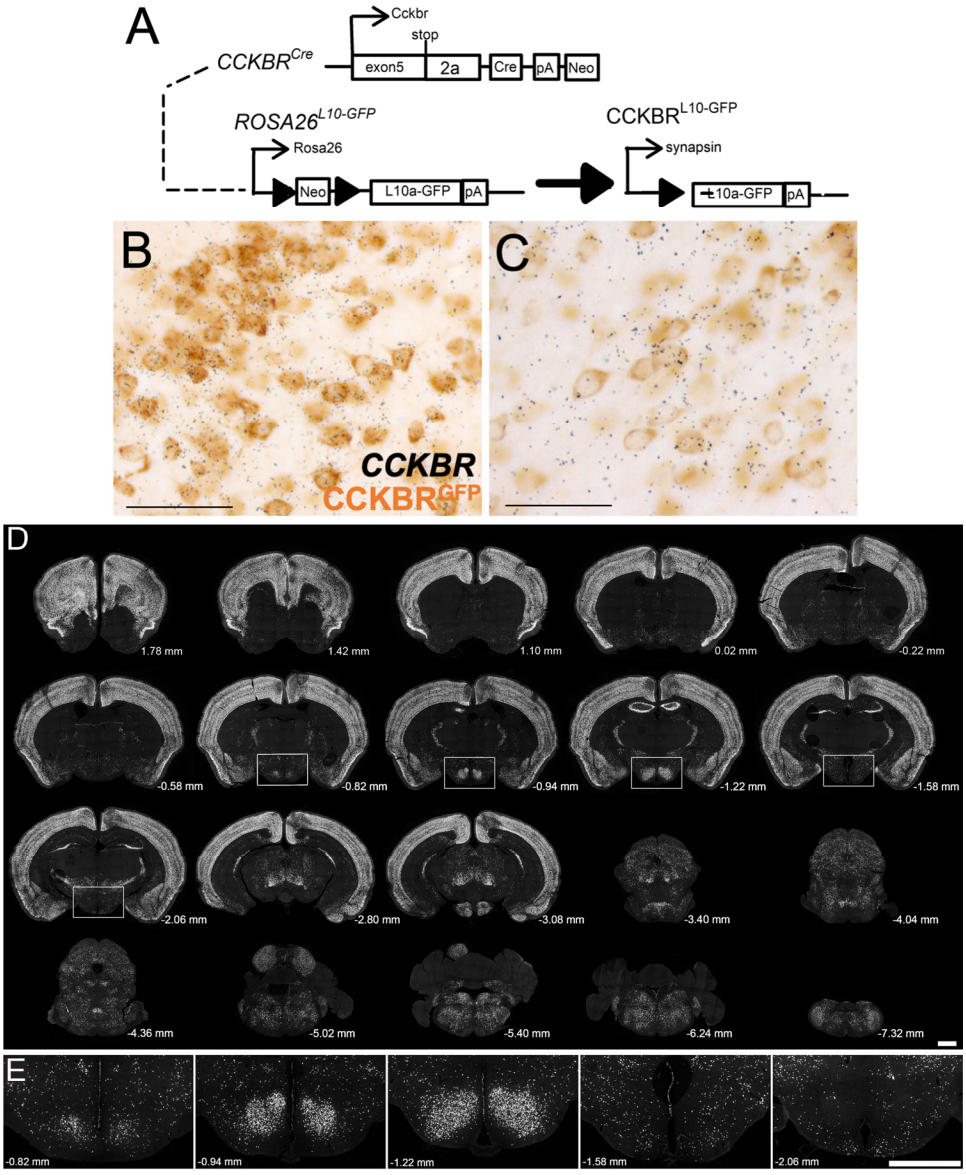

Supplemental Fig. 1. Verification of *Cckbr*^{cre} model. We used *in situ* hybridization for *Cckbr* mRNA and marked cre-containing cells by crossing *Cckbr*^{cre} onto the cre-inducible L10-GFP background (Cckbr$^{eGFP\text{-}L10a}$ mice) (A). We observed *Cckbr* mRNA overlapping GFP-immunoreactivity in sites previously reported to contain dense *Cckbr* expression including the cortex (B) and VMN (C). Scale bars in B-C 100μm; captured at 40x objective. (D) Shows representative images of Cckbr-GFP (white) over the whole brain in coronal sections at the given distances from bregma. Scale bar =1 mm. (E) Shows zoomed images of the ventral medial hypothalamic area at the indicated distances from bregma; scale bar= 1 mm.

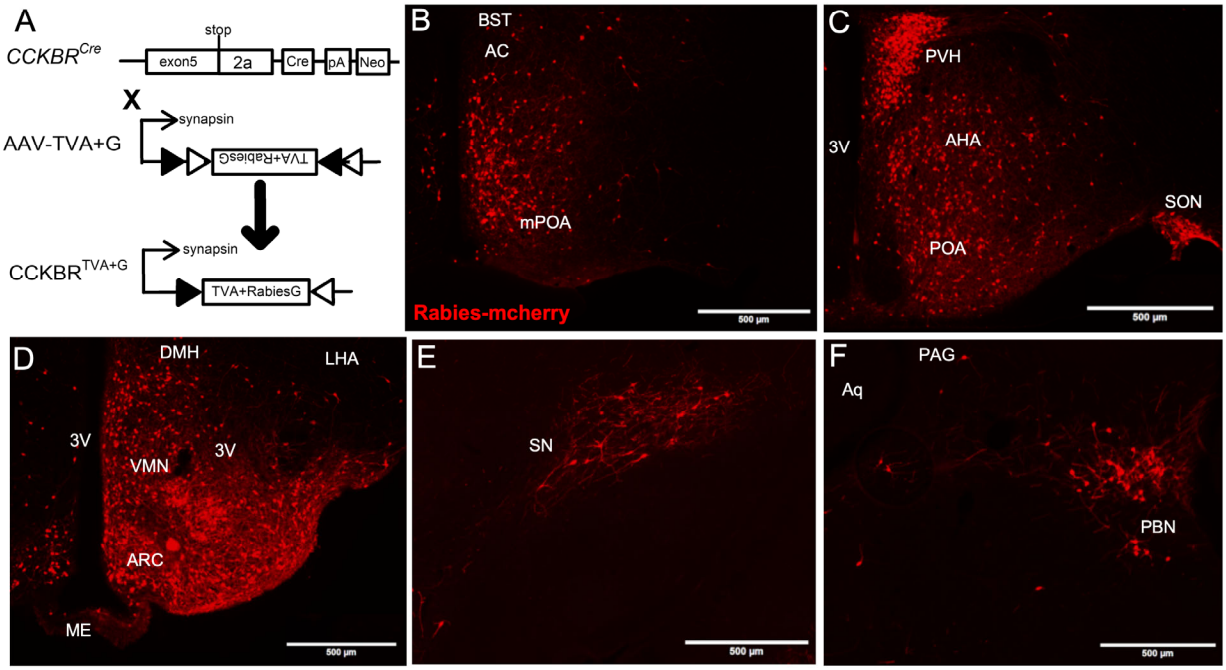

Supplemental Fig. 2. Identification of afferents to VMN^{CCKBR} neurons. (A) Helper virus (AAV^{TVA+G}) was injected into the VMN of *Cckbr^{cre}* mice; 3-6 weeks later, pseudotyped mCherry-expressing rabies virus was injected into the BST (n=3). One week after pseudotyped rabies virus, we perfused the mice and stained for mCherry. Representative images revealed afferent neurons in the (B) POA, (C) AHA and PVH, (D) DMH and ARC, (E) SN, and (F) PBN. Scale bars=500 µM.

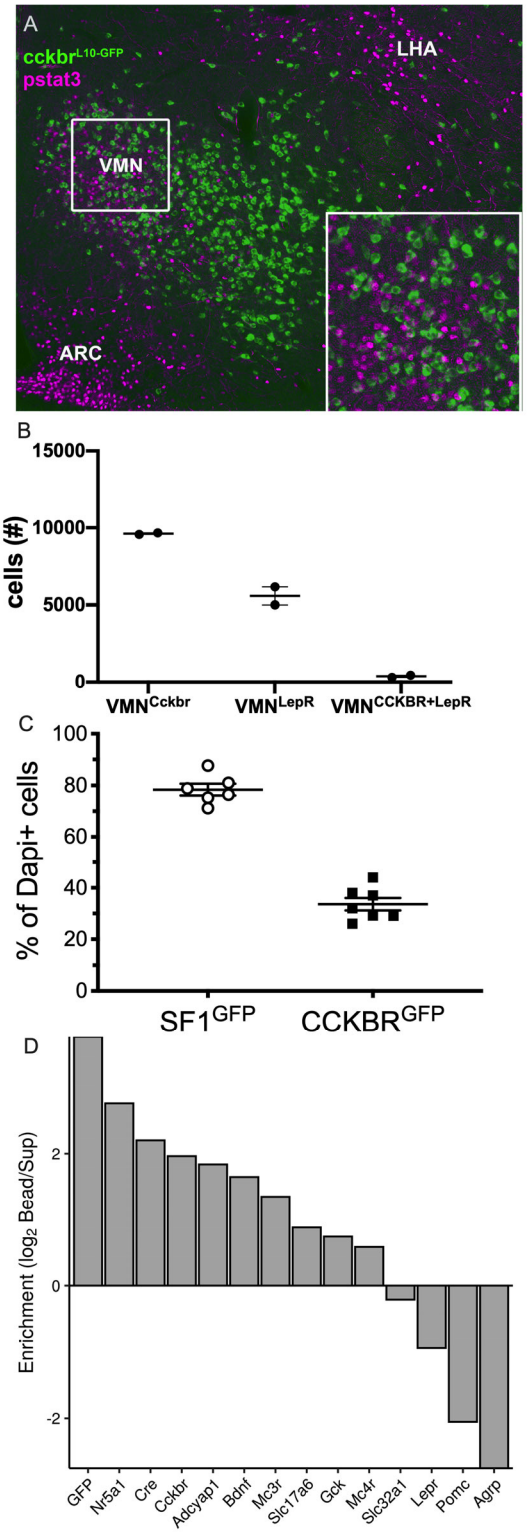

Supplemental Fig. 3. Relationship between VMN^{CCKBR} and other VMN neurons. We treated CCKBR^{GFP} mice with leptin (5 mg/kg, IP, 1 hour) and perfused them. We stained for GFP (green) to identify VMN^{CCKBR} cells and phosphorylated STAT3 (pSTAT3, purple) to identify cells that contain the leptin receptor. A representative image is shown in (A). Image collected at 10x. (B) Quantification of GFP-, pSTAT3-, and

dual-labelled neurons; n=2. (B, C) Mean +/- SEM is shown, with individual data points superimposed; n=6 (SF1), n=7 (CCKBR). (D) Average enrichment of the indicated transcripts from TRAP-seq analysis is shown (log_2(Fold Beads/Sup)). Based upon n=4 replicates.

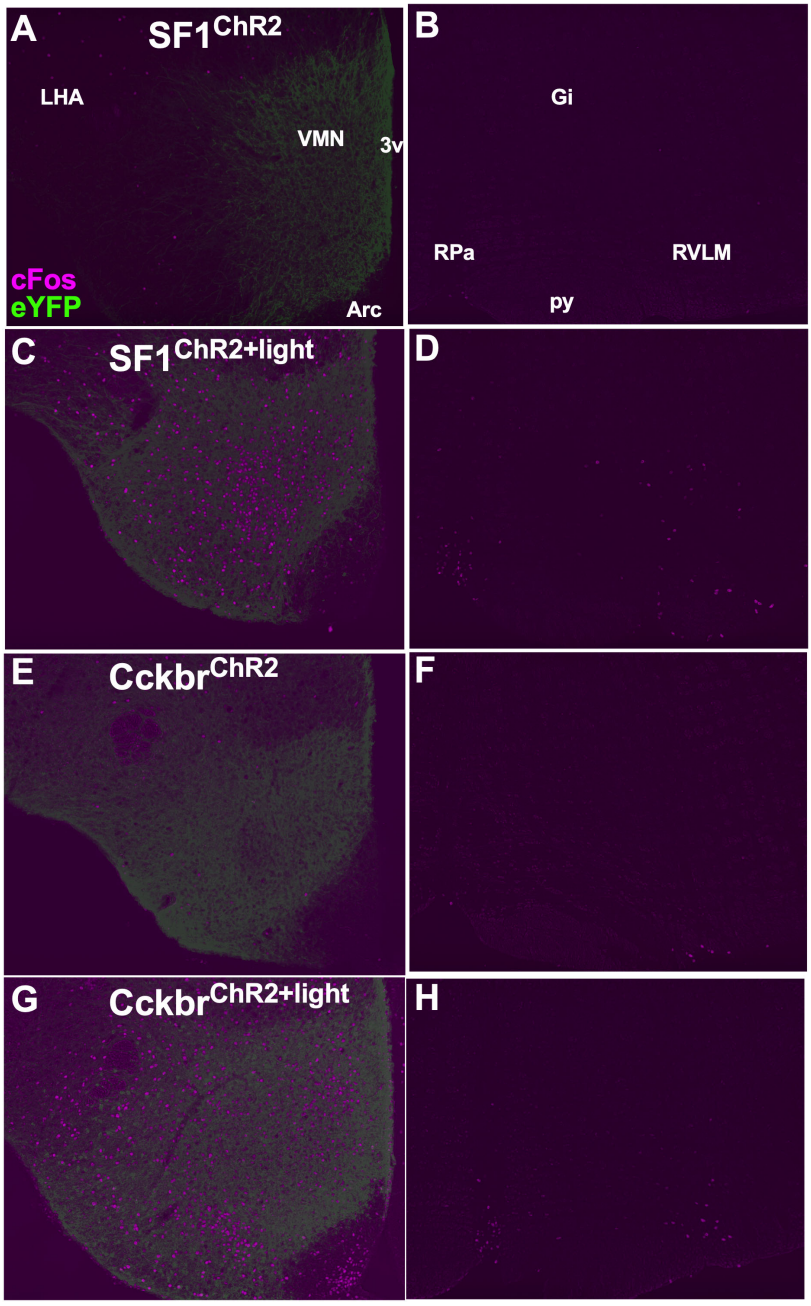

Supplemental Fig. 4. Expression of ChR2-eYFP and activation of FOS-immunoreactivity in SF1^{TT} and CCKBR^{TT} mice (From Figure 1). Mice were perfused and brains were collected 1 hour after the onset of optogenetic stimulation (A, B, E, F) or control (C, D, G, H). Representative images show ChR2-eYFP (green) and FOS (purple) in the (left panels) VMN and the the RVLM and Raphe Pallidus (right panels). CCKBR^{ChR2} (A-D, n=3) and SF1^{ChR2} (E-H, n=5) are shown. Images collected at 10x.

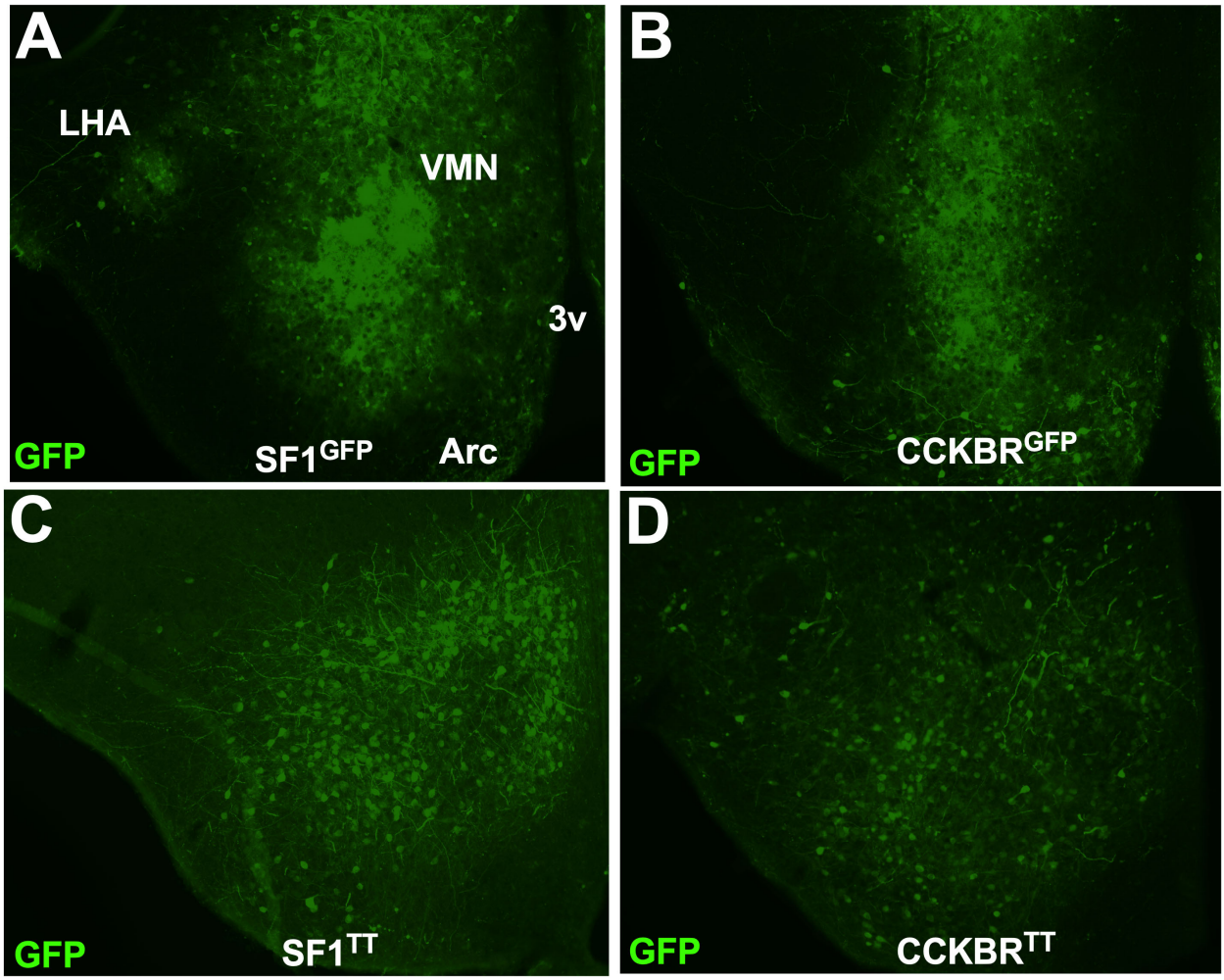

Supplemental Fig. 5. Expression of control (GFP) or TT-eGFP in Sf1^{cre} or Cckbr^{cre} mice (from Figure 2). Representative images showing the immunofluorescent detection of GFP (green) in the VMN region of (A) SF1^{GFP}, (B) CCKBR^{GFP}, (C) SF1^{TT}, and (D) CCKBR^{TT} mice. Images collected at 10x.

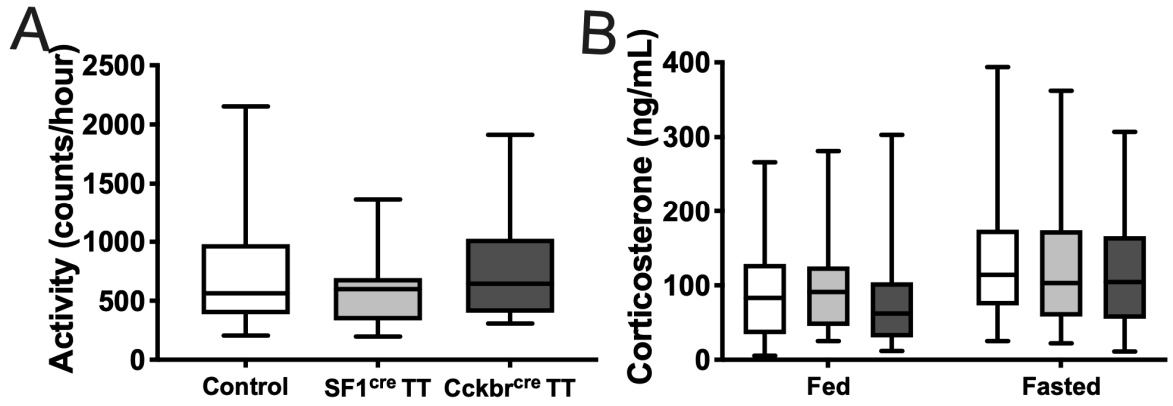

Supplemental Fig. 6. Silencing either all VMN cells using *Sf1*^{cre} (SF1^{TT}) or VMN^{CCKBR} neurons using *Cckbr*^{Cre} (CCKBR^{TT}) did not alter either activity or corticosterone levels (from Figure 2). Data are given as box and whiskers plots that show spread of the data from minimum to maximum, median, first quartile, and third quartile. Data was analyzed by either Two way Repeated Measures ANOVA with Fisher's LSD post hoc test. No significant differences were detected.

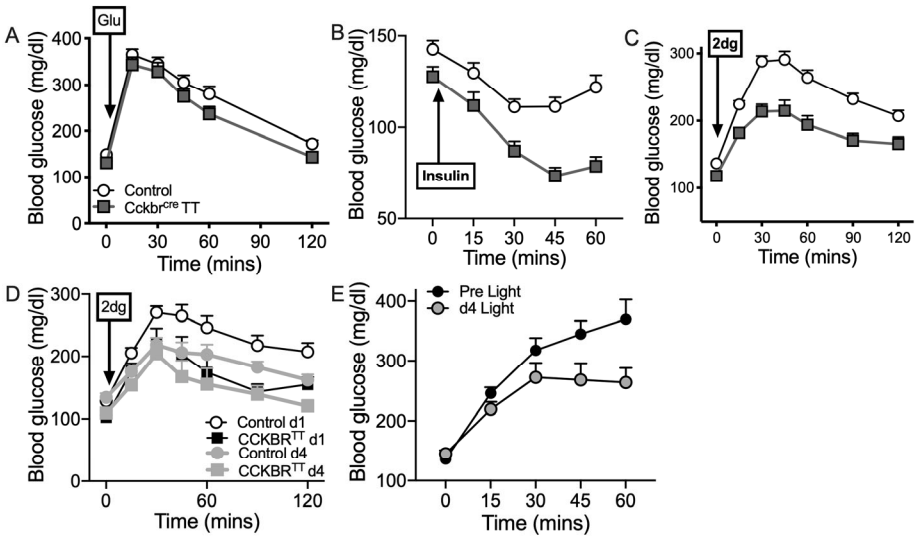

Supplemental Fig. 7. Raw Blood Glucose Values from Figures 5 and 6. (A) Data from Figure 5A. (B-E) Data from Figure 6A-D, respectively. Data are expressed as mean +/- SEM; replicates and statistics were as noted in the main figure.

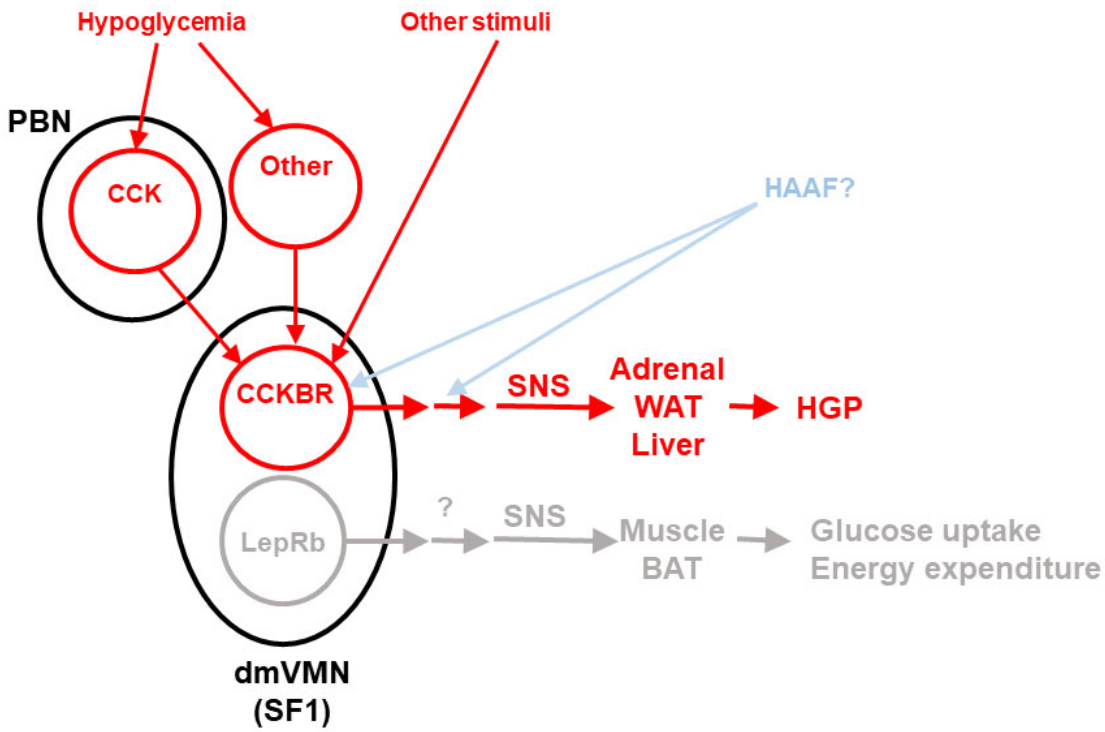

Supplemental Fig. 8. Model for VMN neurons that control blood glucose. Cartoon diagram showing inputs to VMN^{CCKBR} cells that convey information about low glucose (via PBN CCK cells and other hypoglycemia-actived neurons) as well as other signals that indicate the need to increase blood glucose. VMN^{CCKBR} cells promote SNS outflow to increase nutrient mobilization (presumably via the liver, adrenal and white adipose tissue (WAT)), thereby increasing blood glucose concentrations. In contrast, VMN LepRb neurons do not increase blood glucose (2), but may rather promote SNS outflow to skeletal muscle and brown adipose tissue (BAT) to increase glucose uptake and energy expenditure via these tissues (17).